



City Research Online

City St George's, University of London

Citation: Gong, J., Li, Y., Cui, M., Yan, S. & Ma, Q. (2022). Study on the surf-riding and broaching of trimaran in oblique stern waves. *Ocean Engineering*, 266(4), 112995. doi: 10.1016/j.oceaneng.2022.112995

This is the accepted version of the paper.

This version of the publication may differ from the final published version. To cite this item please consult the publisher's version.

Permanent repository link: <https://openaccess.city.ac.uk/id/eprint/29463/>

Link to published version: <https://doi.org/10.1016/j.oceaneng.2022.112995>

Copyright and Reuse: Copyright and Moral Rights remain with the author(s) and/or copyright holders. Copies of full items can be used for personal research or study, educational, or not-for-profit purposes without prior permission or charge, unless otherwise indicated, provided that the authors, title and full bibliographic details are credited, a hyperlink and/or URL is given for the original metadata page and the content is not changed in any way. For full details of reuse please refer to [City Research Online policy](#).

Ocean Engineering

Study on the surf-riding and broaching of trimaran in oblique stern waves

--Manuscript Draft--

Manuscript Number:	OE-D-22-02562R2
Article Type:	VSI: Hybrid Modelling in WSI
Section/Category:	
Keywords:	Trimaran; oblique stern waves; surf-riding; broaching; autopilot
Corresponding Author:	Yunbo Li, PhD Shanghai Maritime University Shanghai, CHINA
First Author:	Jiaye Gong, Doctor
Order of Authors:	Jiaye Gong, Doctor Yunbo Li, PhD Meng Cui, Master Shiqiang Yan, Doctor Qingwei Ma, Doctor
Abstract:	<p>The trimaran is a high-performance ship of excellent seakeeping performance and stability, which makes it less vulnerable to capsizing. In recent years, strong survivability has increased the applicability of trimaran in unmanned ships. However, compared with the stability and seakeeping, side hulls and the larger width make the trimaran's maneuverability not as good as the traditional monohull. The unified study on trimaran's course keeping and broaching in waves is still limited. In this paper, the navigation of trimaran in oblique stern waves is simulated, and the force and moment by the water-jet impetus and nozzle reflection are simplified. The hybrid method coupling FNPT and CFD is applied to simulate the process of surf-riding and broaching. The characteristics of the surf-riding and broaching of the autopilot trimaran in oblique stern waves are analyzed by changing the working condition of initial forward speed, wave parameters, and initial wave heading.</p>
Suggested Reviewers:	<p>Venkatachalam Sriram, Doc. Associate Professor, Indian Institute of Technology Madras vsriram@iitm.ac.in He is well known experts in this area and has carried out research on Hybrid method.</p> <p>Rui Deng, Doc. Professor, Sun Yat-Sen University dengrui_fluid@126.com He has carried out research on trimaran hydrodynamics for many years.</p> <p>Zhijia Xie, Doc. Professor, Cardiff University zxie@cardiff.ac.uk He has carried out research on Wave-Structure Interactions for many years.</p>

Study on the surf-riding and broaching of trimaran in oblique stern waves

Jiaye Gong¹, Yunbo Li^{1*}, Meng Cui², Shiqiang Yan³, Qingwei Ma³

1. College of Ocean Science and Engineering, Shanghai Maritime University, Shanghai, China

2. Marine Design & Research Institute of China, Shanghai, China, 200011

3. School of Mathematics, Computer Science and Engineering, City, University of London, UK

*Corresponding Author: liybsmu@163.com

Abstract: The trimaran is a high-performance ship of excellent seakeeping performance and stability, which makes it less vulnerable to capsizing. In recent years, strong survivability has increased the applicability of trimaran in unmanned ships. However, compared with the stability and seakeeping, side hulls and the larger width make the trimaran's maneuverability not as good as the traditional monohull. The unified study on trimaran's course keeping and broaching in waves is still limited. In this paper, the navigation of trimaran in oblique stern waves is simulated, and the force and moment by the water-jet impetus and nozzle reflection are simplified. The hybrid method coupling FNPT and CFD is applied to simulate the process of surf-riding and broaching. The characteristics of the surf-riding and broaching of the autopilot trimaran in oblique stern waves are analyzed by changing the working condition of initial forward speed, wave parameters, and initial wave heading.

Key Words: trimaran; oblique stern waves; surf-riding; broaching; autopilot

1 Introduction

As one of the high-performance ships, trimaran has the characteristics of high speed, large deck area, excellent performance of stability, and seakeeping. In recent years, by taking advantage of survivability, the trimaran has been gradually used as unmanned vehicles, such as the sea hunter of the USA and the corresponding hull form of China. As we know, compared with the catamaran and the traditional monohull, the trimaran is of relatively low resistance at high speed, and the layout of the two side hulls makes the trimaran not vulnerable to capsizing when sailing in waves (Pattison et al., 1994). However, the side hulls will also lead to the strong nonlinearity of the seakeeping performance of trimaran in different wave headings (Gong et al., 2020, 2021). Furthermore, the larger waterline width of the trimaran will reduce the maneuverability of changing heading (Yasukawa et al., 2005; Gong et al., 2019), and the maneuver in waves is relatively more complicated for the wide range of sailing speed (Gong et al., 2022). Hence, the navigation of the trimaran in waves is a unified problem of both seakeeping and maneuverability, and the corresponding study is still limited.

1
2 Especially for the stern and oblique waves, the surf-riding and broaching is a crucial problem for the
3
4 course keeping and safety of the trimaran's navigation, which deserves more attention and study.

5
6 The International Maritime Organization promulgated Second Generation Intact Stability Criteria
7
8 in 2019, where surf-riding/broaching was listed as one of the five stability failure modes (IMO, 2019).
9
10 The instability problem of surf-riding and broaching concerned by the IMO is closely related to the
11
12 navigation safety of ships in stern and oblique stern waves, especially for ships of high speed and
13
14 small size. The surf-riding indicates that the ship is accelerated or slowed down by the stern or oblique
15
16 stern waves to sail at the same speed as the waves. Furthermore, the surf-riding is usually the
17
18 precondition of broaching (Begovic et al., 2018), which is extremely dangerous for navigation as the
19
20 loss of steerage and abrupt turning.

21
22 The surf-riding and broaching of ships began attracting researchers' attention as early as the 1980s.
23
24 Renilson et al. (1982) began to study the phenomenon of broaching and the corresponding loss of
25
26 sailing direction control in the following severe seas. Then, Renilson (1998) proposed the definition
27
28 of broaching and the analysis method by a non-linear mathematical model. Umeda et al. (2000)
29
30 classified the capsizes of ships into four modes. The nonlinear dynamics method was applied to study
31
32 the qualitative and quantitative characteristics of broaching and low cycle resonance, which was two
33
34 of the four modes. Walree (2002, 2011) began to apply a time domain panel code to simulate the
35
36 navigation of a high-speed petrol boat in stern-quartering seas. The results showed that the proposed
37
38 method could be used to investigate dynamic stability and course keeping in stern quartering seas. In
39
40 the past few years, the surf-riding and broaching of ships in stern and oblique waves still attracted
41
42 many researchers' attention. Spyrou et al. (2016) combined a linear mathematical model of the yaw
43
44 and sway motion with a nonlinear surge equation to predict the high run incidents and broaching
45
46 behavior of a ship in irregular oblique stern waves. Gu et al. (2018) presented the vulnerability criteria
47
48 for surf-riding and broaching. The vulnerability criteria were applied for a tumblehome vessel in the
49
50 stern and oblique stern waves, and the results of the vulnerability criteria were compared with the
51
52 tank test results for validation. Rajendran et al. (2019) applied strip theory to calculate the Froude-
53
54 Krylov and hydrostatic force of a ship in waves. The surf-riding and broaching of a fishing vessel in
55
56 regular astern waves are predicted by the numerical method, and the computed results are compared
57
58 with the experimental results for validation. Weems et al. (2020) developed a split-time method to
59
60 study the broaching and capsizing of the ship in random irregular waves, by which the prediction of
61
62 capsizing was divided into the upcrossing of an intermediate motion threshold and the probability of
63
64 capsizing after up-crossing. The ship navigation was simulated by calculating the nonlinear wave
65

forces and hydrostatic restoring forces separately. Yu et al. (2021) applied a 6DOF numerical model to simulate the navigation of a fishing vessel in the stern and oblique stern waves. By changing the GM of the fishing vessel, the significant influence of GM value on the occurrence of broaching and capsizing was shown. Angelou et al. (2021) presented a mathematical model to assess the tendency for broaching-to of a sailing yacht. By the mathematical model, the maneuvering reaction, hydrostatic forces, wave forces, and the sails of the yacht are solved by different sub-model, where the sails are obtained by the interpolation tables of the pre-calculated aerodynamic and structural force.

It could be found that the study on the surf-riding and broaching is mainly fixed on the monohull fishing vessel, which has the characteristics of medium or small size, high speed, and large transom stern. The method of separately calculating the hydrostatic and wave force is widely used to predict the navigation and broaching of a ship. Though the two side hulls could increase the ship width and the lateral stability for the trimaran, it will also lead to relatively worse maneuverability and a large transom stern. Besides, the high speed and the medium size will also probably increase the vulnerability of trimaran to the surf-riding and broaching in oblique stern waves. Therefore, the layout of two side hulls will also influence the trimaran's surf-riding and broaching process. Therefore, it is necessary to take the intermittent emergence of the side hulls, green water, and bow diving into account for the numerical simulation of the trimaran.

This paper studies the surf-riding and broaching of an autopilot trimaran in regular oblique stern waves. A hybrid method coupling the fully nonlinear potential flow method and viscous flow method is applied for numerical simulation, which has been widely used for the issues of FSI. The fluid ship interaction and the ship's motion are solved by the viscous flow method, and the process of the surf-riding and broaching could be captured with the nonlinear phenomena taken into account. The trimaran is moving forward at an initial speed and heading. When sailing in the waves, the trimaran moves freely, including surge, sway, heave, roll, pitch, and yaw motion. A semi-empirical model of water jet thrust and steering moment is applied to control the initial heading. By changing the initial speed and wave parameter, the course keeping performance and the characteristics of surf-riding and broaching of the trimaran are studied.

2 Numerical methods

The numerical method for the numerical simulation of the autopilot trimaran is briefly introduced in this section first. Then, the boundary condition and the grid generation are introduced.

2.1 Numerical method

For the surf-riding and broaching of a trimaran, the nonlinear effect, including side hull emergence, bow diving, and transient draft variation, is essential for the numerical simulation. Therefore, the flow near the trimaran is solved by the viscous flow method in the internal domain. Because the heat conduction and exchange of water are neglected, the flow field satisfies the mass conservation and momentum conservation, and the fluid is assumed incompressible with the constant density. The incompressible URANS equations can be expressed as

$$\nabla \cdot \mathbf{U} = 0 \quad (1)$$

$$\frac{\partial(\rho \mathbf{U})}{\partial t} + \nabla \cdot [\rho(\mathbf{U} - \mathbf{U}_g)\mathbf{U}] = -\nabla p_d - \mathbf{g} \cdot \mathbf{x} \nabla \rho + \nabla \cdot (\mu_{eff} \nabla \mathbf{U}) + (\nabla \mathbf{U}) \cdot \nabla \mu_{eff} + f_\sigma + f_s \quad (2)$$

Where ρ is density, t is time, \mathbf{g} is the gravitational acceleration, \mathbf{U} is the velocity field, \mathbf{U}_g is the moving velocity of the grid, p_d is the dynamic pressure field, μ_{eff} is the effective dynamic viscosity, f_σ is the surface tension term, f_s is the source term. The VOF and compression techniques are applied to simulate the Euler two-phase flow. An artificial compression technique (Rusche, 2002; Weller, 2002) is used in OpenFOAM to keep the value consecutive and non-zero value only at the interface between air and water.

When the autopilot ship is sailing in the waves, the internal domain moves simultaneously with the ship in the scope of the external domain. The fluid is assumed to be ideal in the external domain, and the velocity potential in the external domain satisfies the Laplace equation. A wavemaker is implemented on one side of the external domain, and a self-adaptive wavemaker is adopted on the other side for wave absorption. Both the kinematic and dynamic boundaries are satisfied on the free surface. The two domains are connected by the interfaces and transition zone. Because the hybrid method has been applied for different issues on FSI, more details about the QALE-FEM and the hybrid method could refer to the reference (Ma et al., 2009; Yan et al., 2010; Hu et al., 2020; Gong et al., 2021).

2.2 Motion of the autopilot trimaran

A global coordinate system (x, y, z) is used for the solution of the flow field, and the force and moment on the ship are obtained in the global coordinate system. When solving the ship's motion, a local coordinate system (x', y', z') is used, whose center overlaps with the gravity center of the trimaran to avoid the force and moment correction. The solution to the 6DOF motion is based on the reference (Xing et al., 2008). The ship's motion could be divided into linear and rotation in the local coordinate system. The linear motion is expressed by the velocity $(u_{x'}, u_{y'}, u_{z'})$ and the corresponding acceleration velocity. The rotation could be expressed by the angular velocity $(r_{x'}, r_{y'}, r_{z'})$ and the

corresponding angular acceleration velocity. The motion and rotation of the trimaran satisfy the 6DOF maneuvering equations

$$\begin{aligned}
m(\dot{u}_{x'}-u_{y'}r_{z'}+u_{z'}r_{y'}) &= F_{Hx'} + F_{WJx'} \\
m(\dot{u}_{y'}-u_{z'}r_{x'}+u_{x'}r_{z'}) &= F_{Hy'} + F_{WJy'} \\
m(\dot{u}_{z'}-u_{x'}r_{y'}+u_{y'}r_{x'}) &= F_{Hz'} + F_{WJz'} \\
I_{x'}r_{x'}+(I_{z'}-I_{y'})r_{y'}r_{z'} &= M_{Hx'} + M_{WJx'} \\
I_{y'}r_{y'}+(I_{x'}-I_{z'})r_{x'}r_{z'} &= M_{Hy'} + M_{WJy'} \\
I_{z'}r_{z'}+(I_{y'}-I_{x'})r_{x'}r_{y'} &= M_{Hz'} + M_{WJz'}
\end{aligned} \tag{3}$$

Where m is the mass of the trimaran, $(I_{x'}, I_{y'}, I_{z'})$ is the inertia moment, $(F_{Hx'}, F_{Hy'}, F_{Hz'})$ and $(M_{Hx'}, M_{Hy'}, M_{Hz'})$ are the total force and moment of the hull surface, which are obtained by the solution of the internal viscous-flow domain in every time step, and the force and moment by the effect of velocity, acceleration velocity, pressure, and viscosity are taken into account. $(F_{WJx'}, F_{WJy'}, F_{WJz'})$ and $(M_{WJx'}, M_{WJy'}, M_{WJz'})$ is the force and moment of the water jet impetus. The rotation is expressed by the Euler angle $(\zeta_4, \zeta_5, \zeta_6)$. After Eq. (3) is solved, the changing rate of the Euler angle could be obtained by

$$\begin{bmatrix} 1 & \sin\zeta_4 \tan\zeta_5 & \cos\zeta_4 \tan\zeta_5 \\ 0 & \cos\zeta_4 & -\sin\zeta_4 \\ 0 & \sin\zeta_4 / \cos\zeta_5 & \cos\zeta_4 / \cos\zeta_5 \end{bmatrix} \begin{bmatrix} \dot{\zeta}_4 \\ \dot{\zeta}_5 \\ \dot{\zeta}_6 \end{bmatrix} \tag{4}$$

For the simulation of the autopilot trimaran, the semi-empirical model of water-jet thrust and steering moment is applied based on the reference (Renilson et al., 1998, Jong et al., 2013). The PD control is used for the autopilot, where the initial heading of 0° is the target, the yaw angle ζ_6 is the error in every timestep, the corresponding angular velocity $\dot{\zeta}_6$ is the changing rate of the error. Hence, the target nozzle deflection angle δ could be obtained by $\delta = K_p \zeta_6 + K_d \dot{\zeta}_6$ in every time step, where $K_p = 9.5$ is the proportional coefficient of the PD control used in this paper, and $K_d = 3.0$ is the differential coefficient of the PD control used in this paper. In this paper, $\delta_{\max} = 35^\circ$ and $\dot{\delta} = 10^\circ/\text{s}$ is used for the autopilot simulation, which means that in every time step the nozzle deflection angle δ will change from the actual value towards the target value at a rate of $10^\circ/\text{s}$.

2.3 Domain and grid generation

The grid of the external FNPT-based QALE-FEM domain is generated based on the reference (Yan et al., 2019). The only difference is that the length of the external domain should be adjusted by the scope of the trimaran's navigation. The autopilot simulation in this paper is similar to the direct maneuver simulation. For the direct maneuver simulation, it is suggested that the typical dimensions of a grid are 3-5 ship lengths in the longitudinal direction, 2-3 in the transverse direction, and one

length in the vertical direction for deep water (ITTC, 2014). Therefore, the internal domain size is $4.5L \times 3.0L \times 2.0L$ in the longitudinal, transverse, and vertical directions. The water domain length above and under water is $0.5L$ and $1.0L$. The meshes of the internal domain are generated by blockMesh and snappyHexMesh, which is the preprocess utilities in OpenFOAM. The grid generation and refinement are similar to the simulation of the zigzag maneuver of trimaran in waves (Gong et al., 2022). The boundary definition of the hybrid method and the grid sketch are shown in Fig. 1.

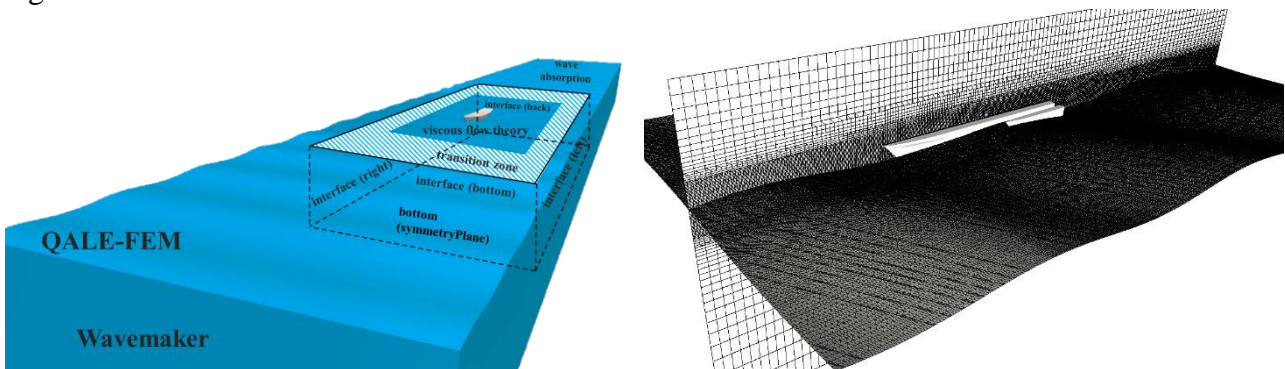


Fig. 1 The sketch of the hybrid method's boundary and the internal domain's grid.

In this paper, the kOmegaSST model was chosen as the turbulent model. The PISO (pressure implicit splitting operator) is used to solve the coupled pressure and velocity fields. As shown in Fig. 1, the internal domain is solved by the viscous flow method. The details of the boundary conditions of the internal domain are shown in Fig. 2. It should be noted that the velocity and volume fraction on the interface is assigned by the external FNPT-based domain, which is solved before the internal domain in every time step (Yan et al., 2019).

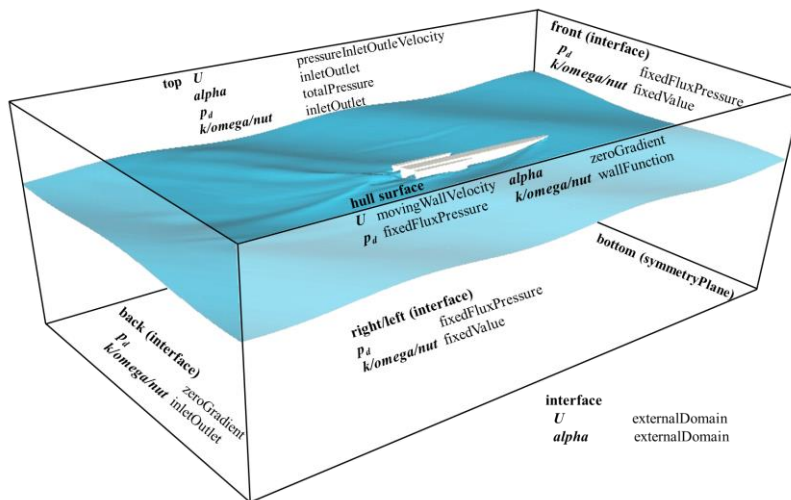


Fig. 2 The sketch of boundary condition and the grid.

3 Validation and verification

In previous work, the hybrid method has been applied and validated for the numerical simulation

of motion in waves and maneuver of trimaran (Gong et al., 2020, 2021, 2022). Hence the validation of the wave generation and navigation in waves is not repeated. The trimaran's navigation in oblique stern waves is autopilot, with the surge, sway, heave, roll, pitch, and yaw took into account. The nozzle deflection angle continuously changes with the in-time heading and heading rate. Therefore, the grid convergence test should be carried out to test the effect of the grid generation on the occurrence of surf-riding and broaching by the current method.

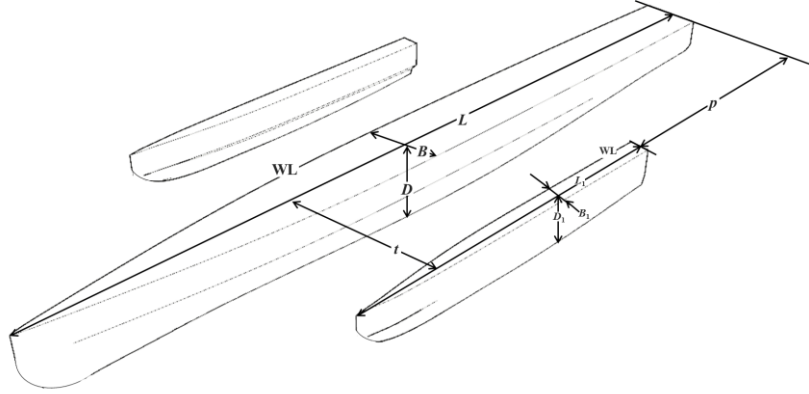


Fig. 3 The sketch of a trimaran and the dimensions

The characteristic dimension of the trimaran form for numerical simulation is as follows: $B/L=0.08$, $D/L=0.04$, $C_b=0.52$, $B_1/L_1=0.05$, $D_1/L_1=0.04$, $C_{b1}=0.46$, $p/L=0.0$, $t/L=0.1$, where L , B , and D are the waterline length, waterline width, and draft of the center hull, L_1 , B_1 , and D_1 are the parameters of the side hull, C_b and C_{b1} are the block coefficient of the center hull and side hull, p and t are the longitudinal and transverse positions of the side hulls as shown in Fig. 3. The wavelength $\lambda/L=1.1$, wave steepness of $ak=0.135$, initial speed $Fr=0.5$, and initial wave heading $\beta=30^\circ$ are used for the test. The time step $dt=T/260$ is used in this paper, where T is the wave period. 80 grids per wavelength and 11 grids per wave height are used for the medium mesh. The ratio $\sqrt{2}$ is used as the grid refinement to refine the background mesh. The coarse, medium, and fine mesh cell numbers are 1.04×10^6 , 2.67×10^6 , and 6.83×10^6 . The computer with a Xeon E5-2650V4 (2.3GHz) cluster and 20 processors are used for the numerical simulation. The three cases are run for $17L^{0.5}$ seconds to make sure the broaching could occur for different mesh schemes. The CPU hours of the coarse, medium, and fine mesh are about 9.5h, 28.2h, and 75.3h, respectively.

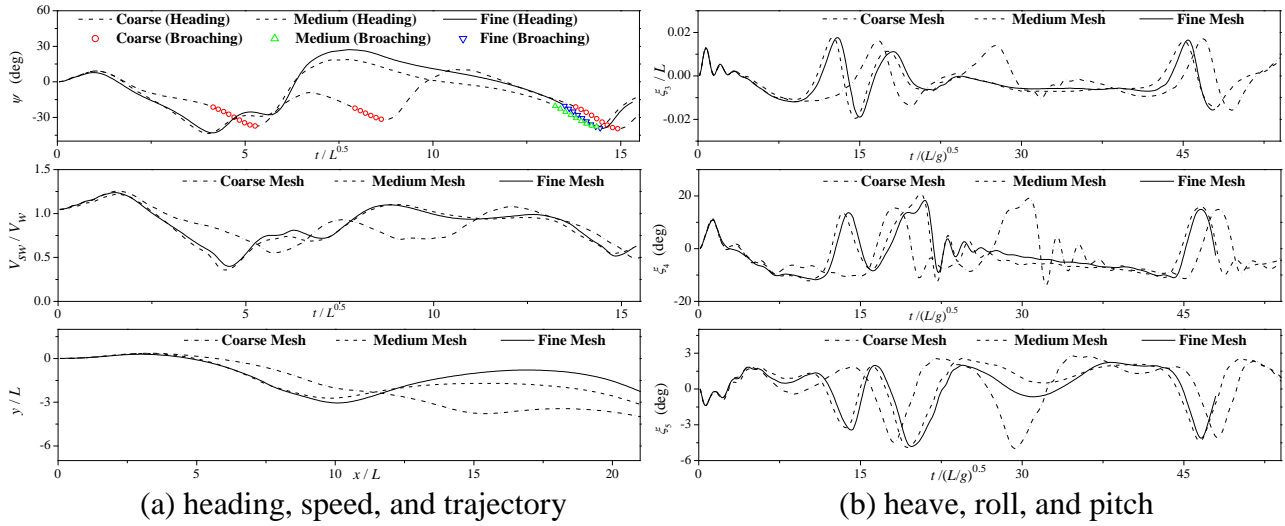


Fig. 4 The computed results by different mesh schemes.

Fig. 4 shows the computed results of the speed and motion by different mesh schemes, where V_{sw} is the projection of in-time ship speed to the wave direction, V_w is the constant wave celerity. The computed result in Fig. 4 shows that when the grid is refined, the time history of the speed and motion by medium and fine mesh are relatively closer to each other. Because the initial position of the trimaran in waves is the same for different cases, it could be noticed that the influence of the mesh scheme is more significant before broaching occurs. The variation trend of the heading and speed by the coarse mesh is entirely different, where two more times of broaching could be observed. However, during $t/\sqrt{L}=13\sim 15$ when broaching occurs for all three mesh schemes, the variation trend of both the speed and motion by different mesh schemes is relatively similar. It probably means that the relative position of the trimaran to the wave during broaching is almost unchanged, which could reduce the requirements for grid density. From the trajectory in Fig. 4 (a), we could also find that the trajectory difference between the three mesh schemes is more noticeable because of the cumulative effect of trajectory errors. The scheme of the medium mesh is used for all the cases hereafter.

4 Results and discussions

In this section, the autopilot trimaran in oblique stern waves is simulated. The effects of wave parameters, initial heading, and forward speed are discussed.

3.1 The effect of wave steepness

Because most of the surf-riding and broaching occurs when sailing in steep waves, the effect of the wave steepness plays an important role in the surf-riding and broaching of monohulls. Hence, the navigation of an autopilot trimaran in oblique stern waves of different steepness is simulated first to study the influence of wave steepness. Aim to study the effect of wave steepness, the wavelength is

kept constant, and the various initial forward speeds of the trimaran are used for the simulation to change the ratio of initial forward speed to wave celerity.

Table 1 The working condition of incident waves and ship

Fr	V_{sw}/V_w	ω_e	ak	λ/L	β
0.35	0.73	1.18			
0.40	0.83	0.73			
0.45	0.94	0.28	0.058		
0.50	1.04	0.17	0.135	1.1	30°
0.55	1.14	0.62			
0.60	1.25	1.07			
0.65	1.35	1.53			

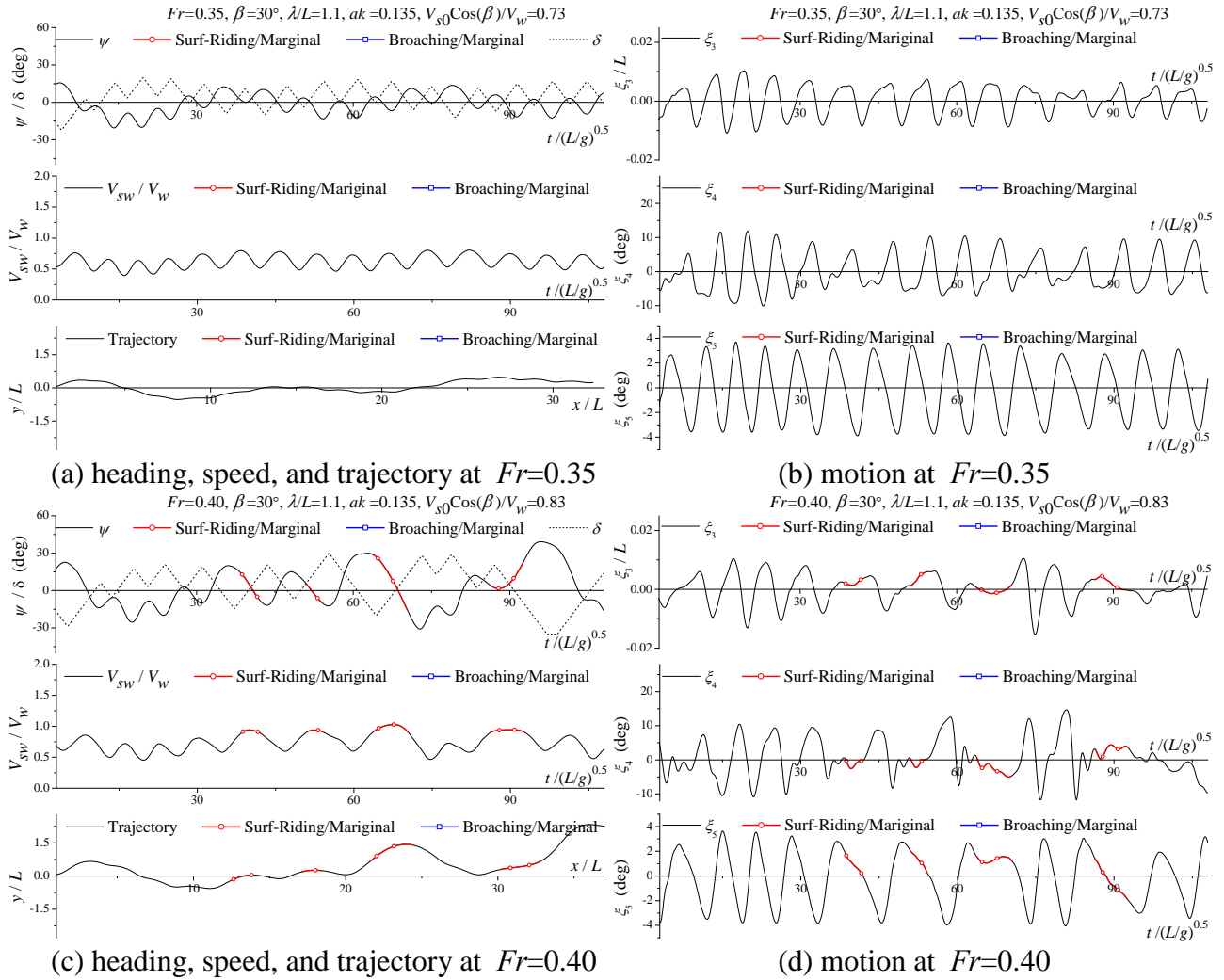
The working conditions are shown in Table 1. Where $Fr=V_{s0}/\sqrt{Lg}$ is the waterline length Froude number, V_{s0} is the initial forward speed of the ship, a is the wave amplitude, k is the wave number, λ is the wavelength, ak means the wave steepness, β is the initial wave heading, $\beta=0^\circ$ means the stern wave in this paper, $V_{sw}=V_{s0}\cos\beta$ is the projection of initial ship speed V_{s0} to the wave direction, V_w is the wave celerity, ω_e is the encounter frequency. In this paper, the marginal surf-riding is judged by $V_{sw}>0.9V_w$, the surf-riding is judged by $V_{sw}=V_w$, the marginal broaching is judged by ($\xi_6>20^\circ$, $\delta=\delta_{\max}$, $\dot{\xi}_6>0$), the broaching is judged by ($\xi_6>20^\circ$, $\delta=\delta_{\max}$, $\dot{\xi}_6>0$, $\ddot{\xi}_6>0$), where $\delta_{\max}=35^\circ$ and $\dot{\delta}=10^\circ/s$ are used (Renilson et al., 1998; Jong et al., 2013).

Table 2 The occurrence of surf-riding and broaching in different wave steepness

Fr	V_{sw}/V_w	$ak=0.058$			$ak=0.135$		
		O_{MS}/O_S	O_{MB}	O_B	O_{MS}/O_S	O_{MB}	O_B
0.35	0.73	×	×	×	×	×	×
0.40	0.83	√	×	×	√	×	×
0.45	0.94	√	×	×	√	√	×
0.50	1.04	√	×	×	√	√	×
0.55	1.14	√	×	×	√	√	√
0.60	1.25	√	×	×	√	×	×
0.65	1.35	√	×	×	√	×	×

The computed results in Table 2 show the occurrence of the surf-riding and broaching when the trimaran sails in oblique stern waves with different wave steepness and initial forward speed, where O_{MS} is the occurrence of marginal surf-riding, O_S is the occurrence of surf-riding, O_{MB} is the occurrence of marginal broaching, O_B is the occurrence of broaching. Table 2 shows that it is easy for the trimaran to be captured by the oblique stern waves, and the results of marginal surf-riding and

surf-riding are similar in different ak . No marginal broaching or broaching appears when the wave steepness is as small as $ak=0.058$. For steep waves of $ak=0.135$, the condition is different. The marginal broaching occurs at V_{sw} close to V_w , and the broaching occurs when V_{sw} is a bit larger than V_w . By comparing the results of $ak=0.058$ and 0.135 , we could notice that large ak is a critical factor for the trimaran's broaching. The Fr where the surf-riding occurs is the same for $ak=0.058$ and 0.135 , but only in $ak=0.135$ will the surf-riding lead to marginal broaching or broaching. Therefore, the time history of the speed and motion of $ak=0.135$ are shown for discussion. In the figures of the time history, the results where the surf-riding and broaching occurs are marked with different symbols separately. In order to facilitate the distinction, the motions of heave, roll, and pitch are expressed by ξ_3, ξ_4, ξ_5 , the heading is expressed by ψ , which is the same to ξ_6 .



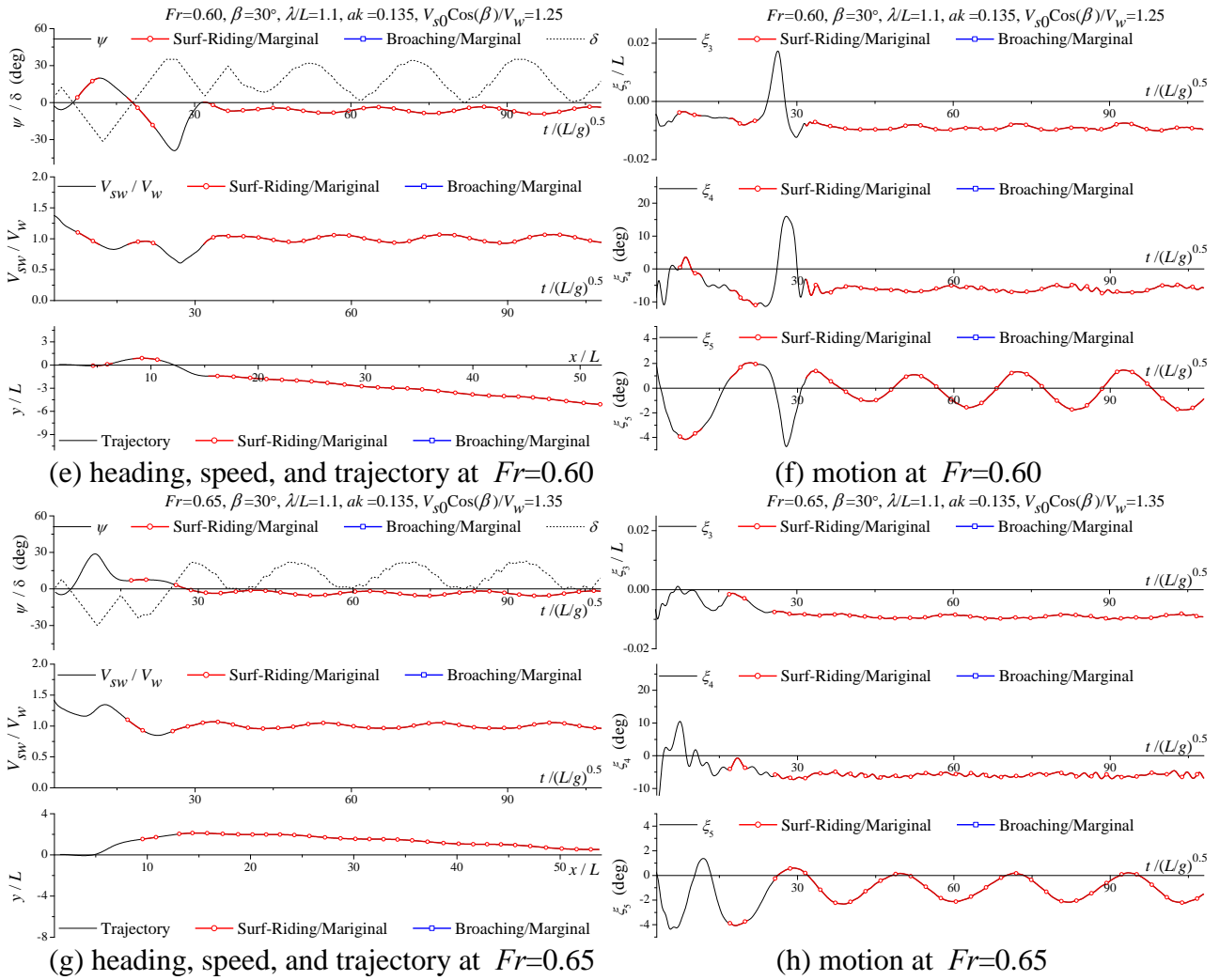


Fig. 5 The time history of computed results at various Fr ($\lambda/L=1.1$, $ak=0.135$, without broaching).

Fig. 5 shows the time history of the autopilot trimaran's speed, motion, and trajectory in oblique stern waves at $Fr=0.35$, 0.40 , 0.60 , and 0.65 , which are the initial speeds no broaching occurs. From Fig. 5 (a)(c)(e)(g), the heading shows that the trimaran is relatively more vulnerable to surf-riding when $V_{sw} > V_w$. It also means that the oblique stern waves are more likely to slow down the trimaran than to accelerate. By comparing Fig. 5 (e) and (g), it could be found that when the initial speed and V_{sw}/V_w increase, the heading of the trimaran is easier to control under the same conditions, and the course deviation is relatively less noticeable. By the motion in Fig. 5 (b)(d)(f)(h), it shows that when the $Fr=0.60$ and V_{sw}/V_w approximates 1.0, an significant motion could be observed after the second surf-riding appears. Combined Fig. 5 (e) and (f), it could be found that when the second surf-riding occurs, the heading deviates from the wave direction, and V_{sw} continues to decrease at the same time. It means that the stern and bow of the trimaran are affected by the wave peak in a short time. When the wave peak is acting on the bow and the V_{sw}/V_w reaches the valley, the value of heave, roll to starboard, and trim by stern is the largest. Whereas, it is probably because the initial projection speed

is not close enough to the wave celerity, the time of the surf-riding before the significant motion is not long enough to lead to broaching.

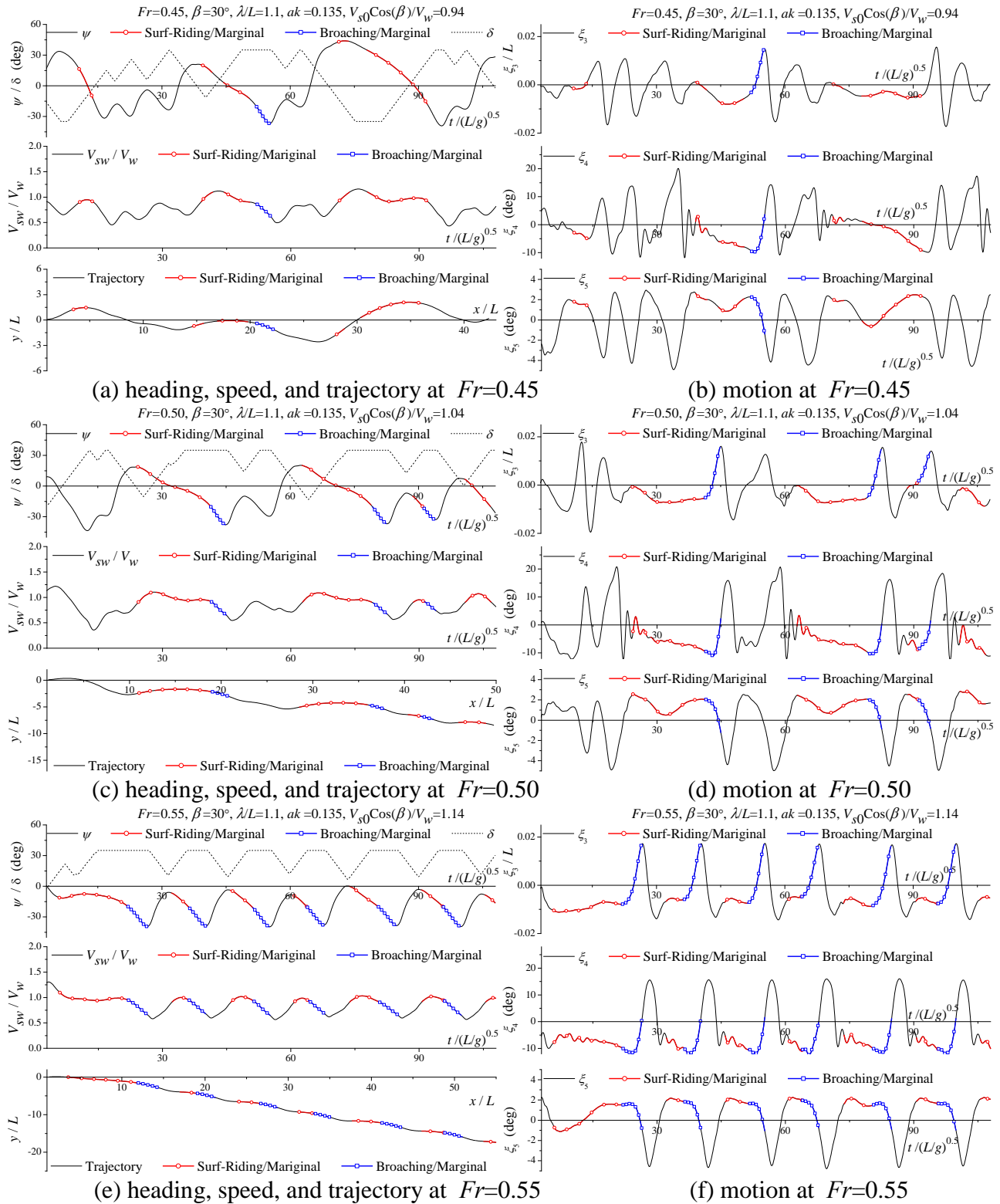
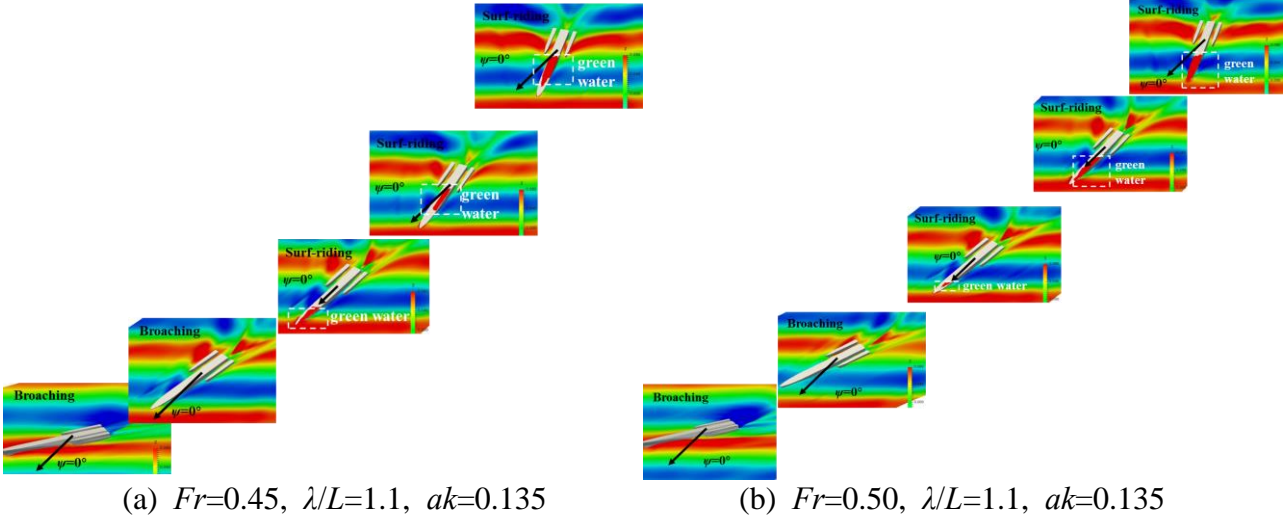


Fig. 6 The time history of computed results at various Fr ($\lambda/L=1.1$, $ak=0.135$, with broaching).

Fig. 6 shows the time history of the autopilot trimaran's speed, motion, and trajectory in oblique stern waves at $Fr=0.45$, 0.50 , and 0.55 , which are the initial speeds at which both surf-riding and

1
2
3
4
5
6
7
8
9
10
11
12
13
14
15
16
17
18
19
20
21
22
23
24
25
26
27
28
29
30
31
32
33
34
35
36
37
38
39
40
41
42
43
44
45
46
47
48
49
50
51
52
53
54
55
56
57
58
59
60
61
62
63
64
65

broaching occur. Fig. 6 (a)(c)(e) shows that the surf-riding and broaching at different initial speeds are similar, and broaching follows the surf-riding. When the state of trimaran varies from surf-riding to broaching, the significant variation of the projection speed V_{sw} could be observed, which is mainly because the trimaran's heading ψ is rapidly moving away from the wave direction. The trajectory shows that the course deviation usually begins when broaching appears, and the course will keep deviating until the next surf-riding. By comparing Fig. 6 (c) and (a)(e), it could be noticed that when the broaching occurs, the V_{sw}/V_w closer to 1.0 will still cause the trimaran to maintain δ_{max} for a longer time to change broaching state. However, the course deviation is still more evident at a higher initial speed. From the motion in Fig. 6 (b)(d)(f), it could be found that no matter how the initial speed changes, the variation trend of the motion during broaching is similar. When broaching happens, the trim by stern could be observed, and the heave becomes positive. The trend of the heave motion means that the surf-riding usually begins when the heave is negative, where the trimaran is in the wave valley. Then, when the wave peak slams on the trimaran from the stern, the heading will change significantly to lead to broaching, during which the heave value changes rapidly from negative to positive by the effect of the wave peak.



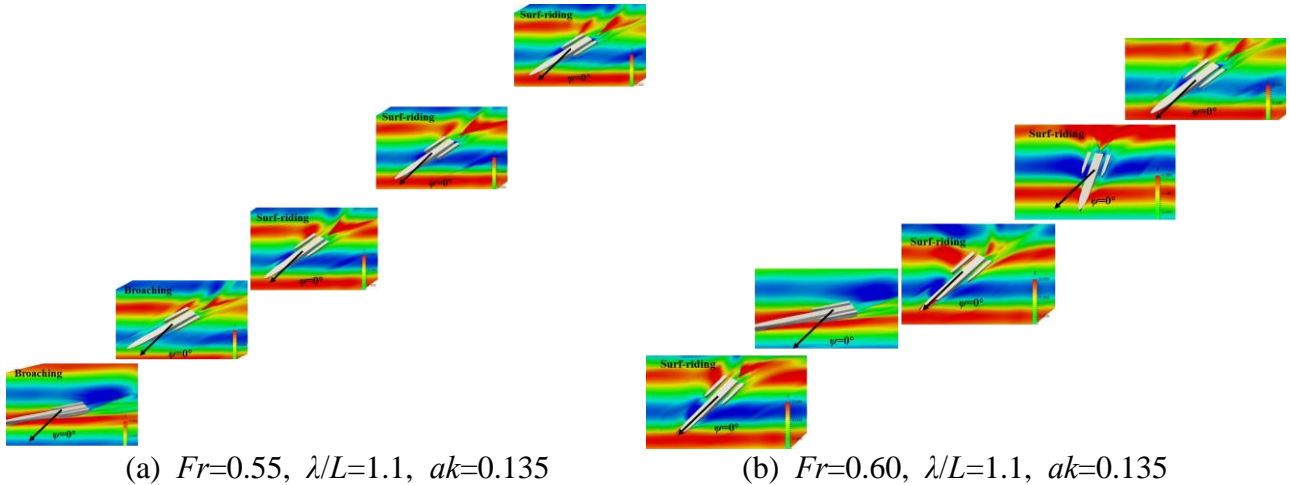


Fig. 7 The wave profile during the simulation at various Fr .

Fig. 7 shows the autopilot trimaran wave profiles in oblique stern waves, and the wave profiles of the first broaching are shown for cases where broaching occurs several times. Fig. 7 shows that the wave celerity V_w is larger than the projection speed V_{sw} at the end of the surf-riding. This time the wave peak is acting on the right side hull of the trimaran. The heading of the trimaran will turn to the starboard sharply by the wave peak. Then, after the wave peak passes the center of the trimaran, the wave peak helps to slow down the deflection of the heading. The largest heading appears when the wave peak reaches the bow side of the trimaran. Such a process is the same for the cases with different initial speeds, which is why the heave, trim by stern, and roll to the starboard reach the peak when the max heading deviation appears. It could also be noticed from Fig. 7 that when the wave peak is at the stern side, the larger wave steepness will make the left side hull of the trimaran sink deeper into the wave. When the wave peak reaches the bow side, the side hulls are almost above water, and the large wave peak could decrease the heading deviation. Therefore, we could predict that the two side hulls may have an opposite influence on the broaching and course deviation, and the side hull position will probably change the characteristics of the autopilot trimaran in stern waves. Fig. 7 also shows that when the initial speed V_{sw} increases, it is relatively more difficult for the waves to change the heading to get larger. Hence, the trimaran will be captured and move together with the waves at the end.

3.2 The effect of wavelength

In this section, the influence of the wavelength on the characteristics of trimaran's surf-riding and broaching is studied. It is noticed that the trimaran is more vulnerable to course deviation and broaching at a high initial speed. Therefore, two initial forward speeds are used for simulation when studying the effect of wavelength on the course keeping and broaching of the trimaran.

Table 3 The working condition of incident waves and ship

λ/L	$Fr=0.35$		λ/L	$Fr=0.45$		ak	β
	V_{sw}/V_w	ω_e		V_{sw}/V_w	ω_e		
0.9	0.80	0.95	1.7	0.75	0.87		
0.8	0.85	0.76	1.5	0.80	0.75		
0.7	0.91	0.45	1.3	0.86	0.57	0.135	30°
0.6	0.98	0.11	1.1	0.94	0.30		
0.5	1.07	0.48	0.9	1.03	0.14		

The working conditions are shown in Table 3. Because the ratio of initial forward speed to wave celerity is sensitive to the variation of wavelength in stern waves, the wavelength used for $Fr=0.45$ is significantly larger than that for $Fr=0.35$ to make sure the variation of V_{sw}/V_w is around 1.0. For all the cases, the initial wave heading is 30°, and the wave steepness is kept constant with $ak=0.135$.

Table 4 The occurrence of surf-riding and broaching in different wavelength

V_{sw}/V_w	$Fr=0.35$			V_{sw}/V_w	$Fr=0.45$		
	O_{MS}/O_S	O_{MB}	O_B		O_{MS}/O_S	O_{MB}	O_B
0.80	×	×	×	0.75	√	√	×
0.85	×	×	×	0.80	√	√	×
0.91	√	×	×	0.86	√	√	×
0.98	√	×	×	0.94	√	√	×
1.07	√	×	×	1.03	√	√	√

The occurrence of surf-riding and broaching in different wavelengths are shown in Table 4. Though the variation of the wavelength could make the V_{sw} vary up and down the V_w , there is no broaching or marginal broaching when the trimaran sails at a low initial speed $Fr=0.35$, and the surf-riding only occurs in a relatively small range of speed. When the trimaran sails at a high initial speed of $Fr=0.45$, it is evident that the trimaran is more vulnerable to surf-riding and broaching. The surf-riding and marginal broaching happen over the entire range of simulated wavelength, and the broaching occurs in the wavelength whose wave celerity is a bit smaller than the ship projection speed with $V_{sw}/V_w=1.03$. It could be seen that the V_{sw}/V_w close to 1.0 is more probable to lead to broaching, but the high speed will still play an essential role in the trimaran's navigation in oblique stern waves.

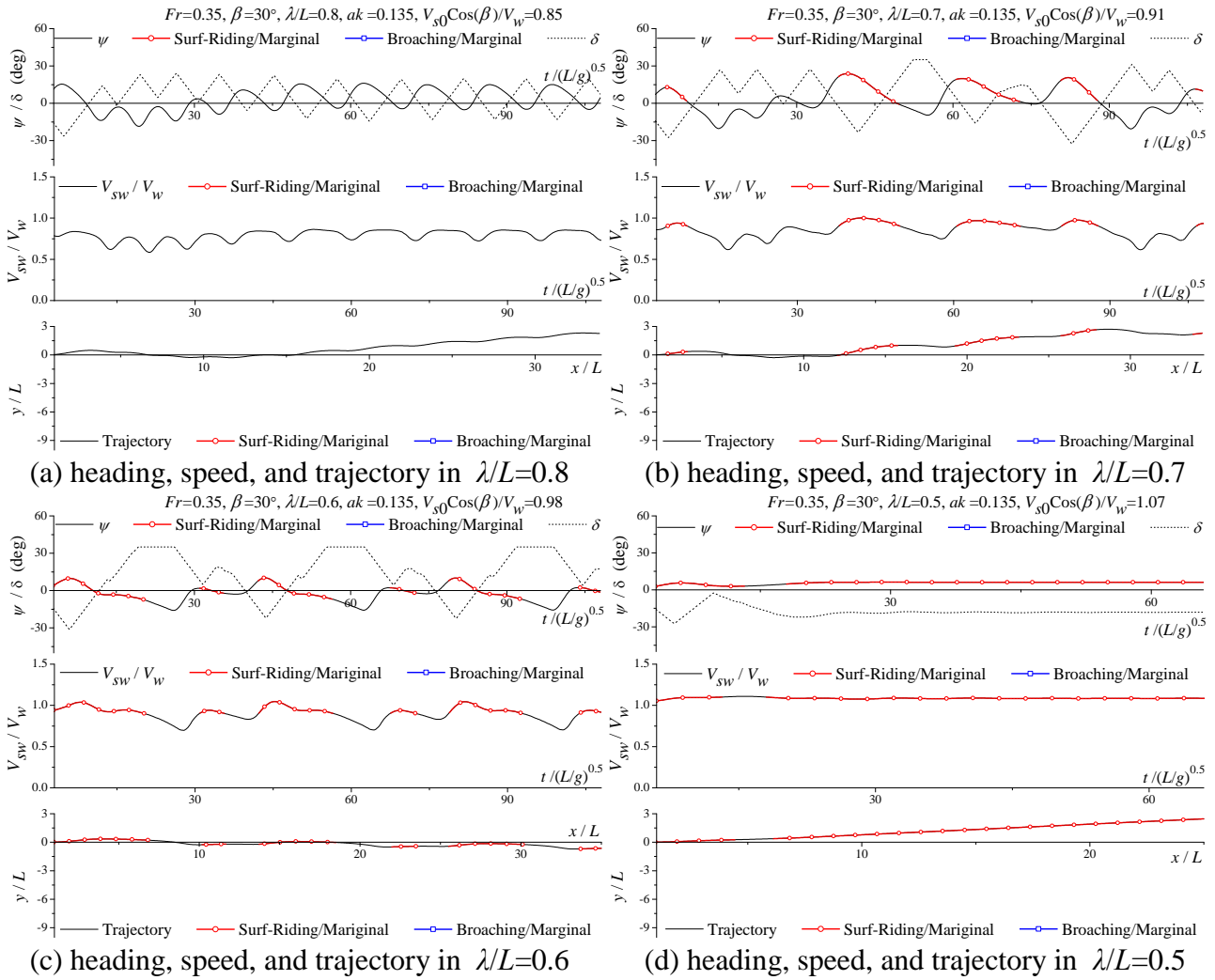
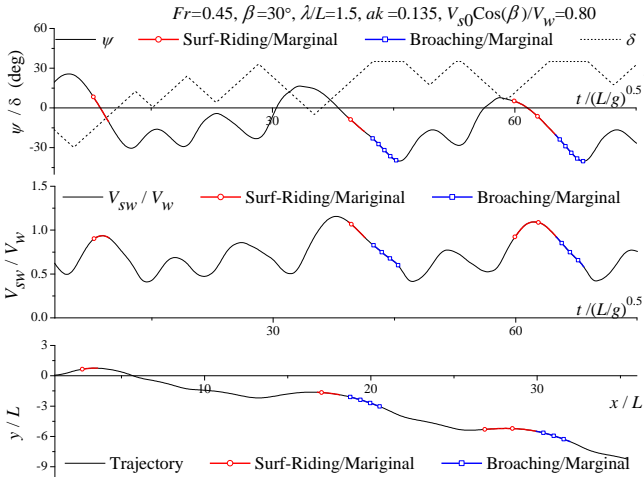


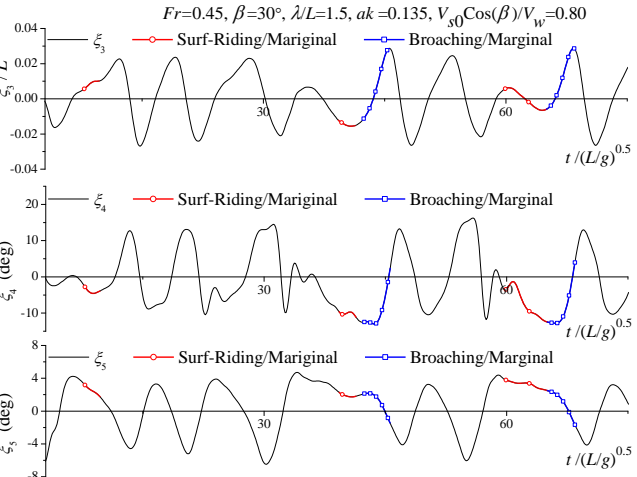
Fig. 8 The time history of computed results in various λ/L ($ak=0.135$, $Fr=0.35$).

Fig. 8 shows the heading variation, the speed variation, and the trajectory deviation of the trimaran at initial speed $Fr=0.35$. It could be found that no broaching occurs during the autopilot process. The surf-riding happens when $V_{sw}/V_w \geq 0.91$. Especially in short waves of $V_{sw}/V_w=1.07$, the trimaran is entirely captured and moves together with the waves with a constant heading and rudder angle. Though no broaching appears for all cases, the wavelength with $V_{sw}/V_w=0.98$ is still relatively more difficult for heading control, where the time for the max rudder angle to appear is the longest. By comparing Fig. 8 (b)(c) and (d), it probably could be predicted that when the trimaran is sailing at a medium speed $Fr=0.35$ with the initial projection speed V_{sw} close to the wave celerity V_w , it is relatively easier for the waves with $V_w < V_{sw}$ to decrease the speed of trimaran to reach surf-riding. The trimaran at an initial medium speed is not easy to be accelerated by the waves to a state of surf-riding when V_w is slightly larger than V_{sw} .

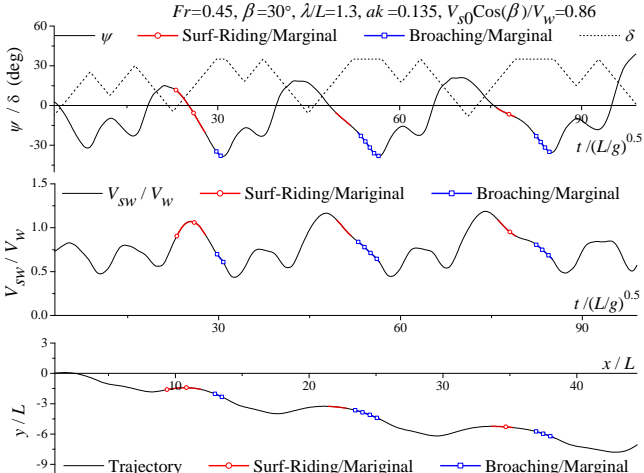
1
2
3
4
5
6
7
8
9
10
11
12
13
14
15
16
17
18
19
20
21
22
23
24
25
26
27
28
29
30
31
32
33
34
35
36
37
38
39
40
41
42
43
44
45
46
47
48
49
50
51
52
53
54
55
56
57
58
59
60
61
62
63
64
65



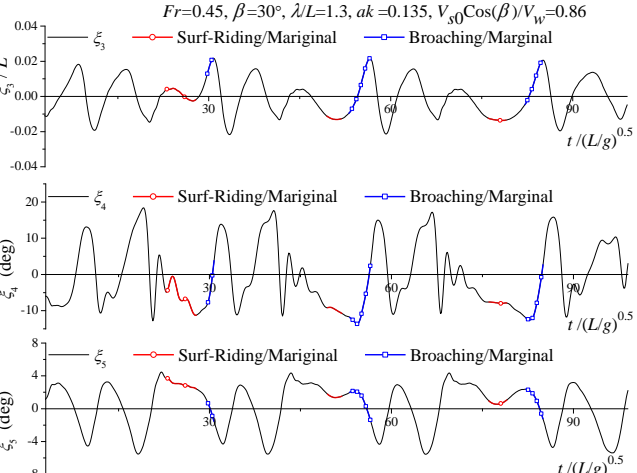
(a) heading, speed, and trajectory in $\lambda/L=1.5$



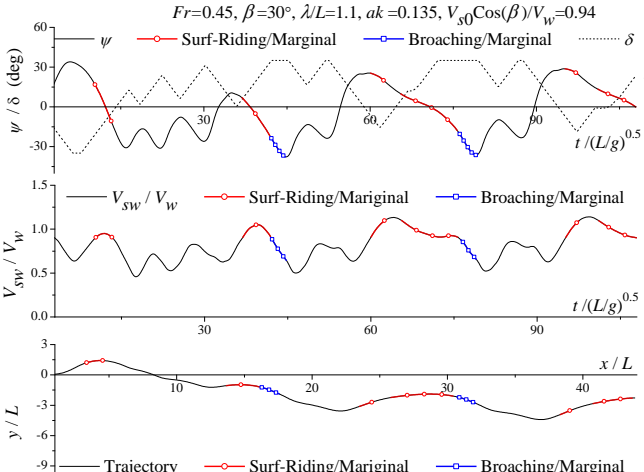
(b) motion in $\lambda/L=1.5$



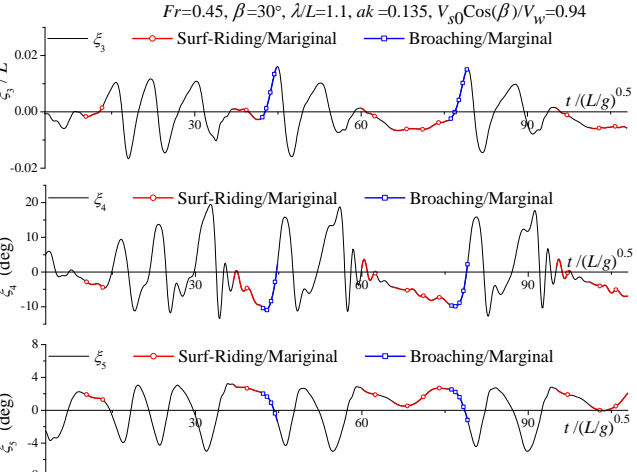
(c) heading, speed, and trajectory in $\lambda/L=1.3$



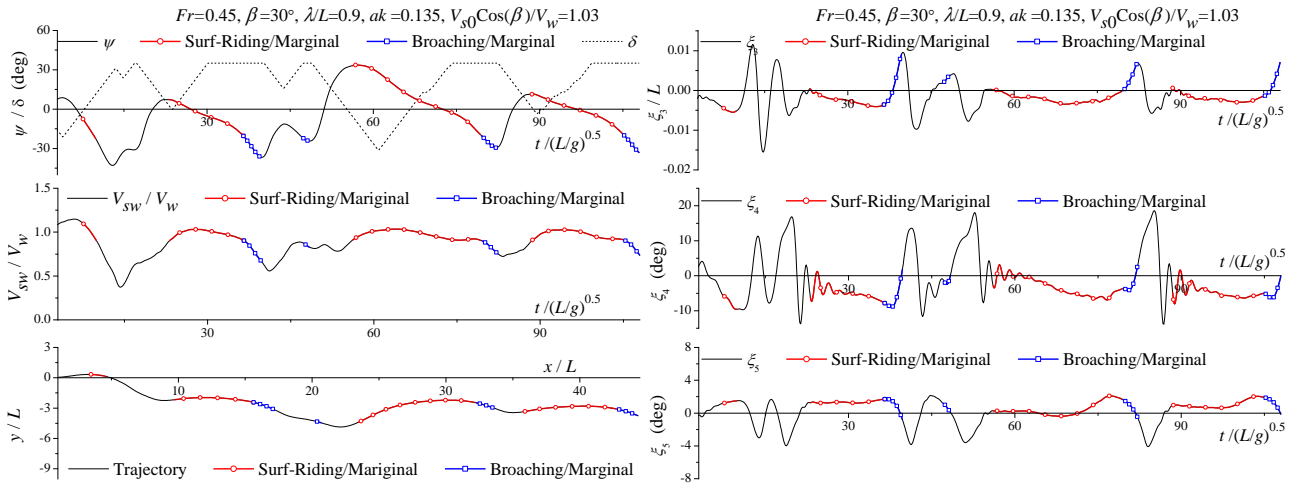
(d) motion in $\lambda/L=1.3$



(e) heading, speed, and trajectory in $\lambda/L=1.1$



(f) motion in $\lambda/L=1.1$



(g) heading, speed, and trajectory in $\lambda/L=0.9$

(h) motion in $\lambda/L=0.9$

Fig. 9 The time history of computed results in various λ/L ($ak=0.135$, $Fr=0.45$).

When the trimaran moves at a high initial speed of $Fr=0.45$, the λ/L ranging from 1.7 to 0.9 could lead to marginal broaching or broaching. Fig. 9 shows the speed, motion, and trajectory in various λ/L at $Fr=0.45$. Similar to the phenomenon at $Fr=0.35$, when the initial speed V_{sw} is close to the wave celerity V_w , the longest time for the max rudder angle is necessary to control the heading of the trimaran, and the course deviation is relatively less noticeable, as shown in Fig. 9 (e)(g). By comparing the surf-riding and broaching in different wavelengths, it could be found that when the V_{sw} gets close to the V_w , the trimaran will experience a longer time of surf-riding before the broaching or marginal broaching occurs, especially for $V_{sw}/V_w=1.03$ is the only case of broaching in Fig. 9 (g). The long-term state of surf-riding is also one of the reasons for slight course deviation. The motion in Fig. 9 (b)(d)(f)(h) shows that the various λ/L will not change the variation trend of the motion during the process of surf-riding and broaching. When broaching occurs in different λ/L , the vertical rise and trim by stern could be observed, which means that no matter how λ/L varies, the trimaran will always move from the downslope to the upslope of the wave during broaching. Besides, the heel angle always changes from portside to starboard during broaching, and the heel is close to zero when broaching ends. It means the wave force is positive to make the trimaran back upright during broaching. By comparing the peak value of the motion, it could be noticed that the λ/L will only obviously influence the peak value of heave during broaching, which gets smaller with the λ/L getting shorter.

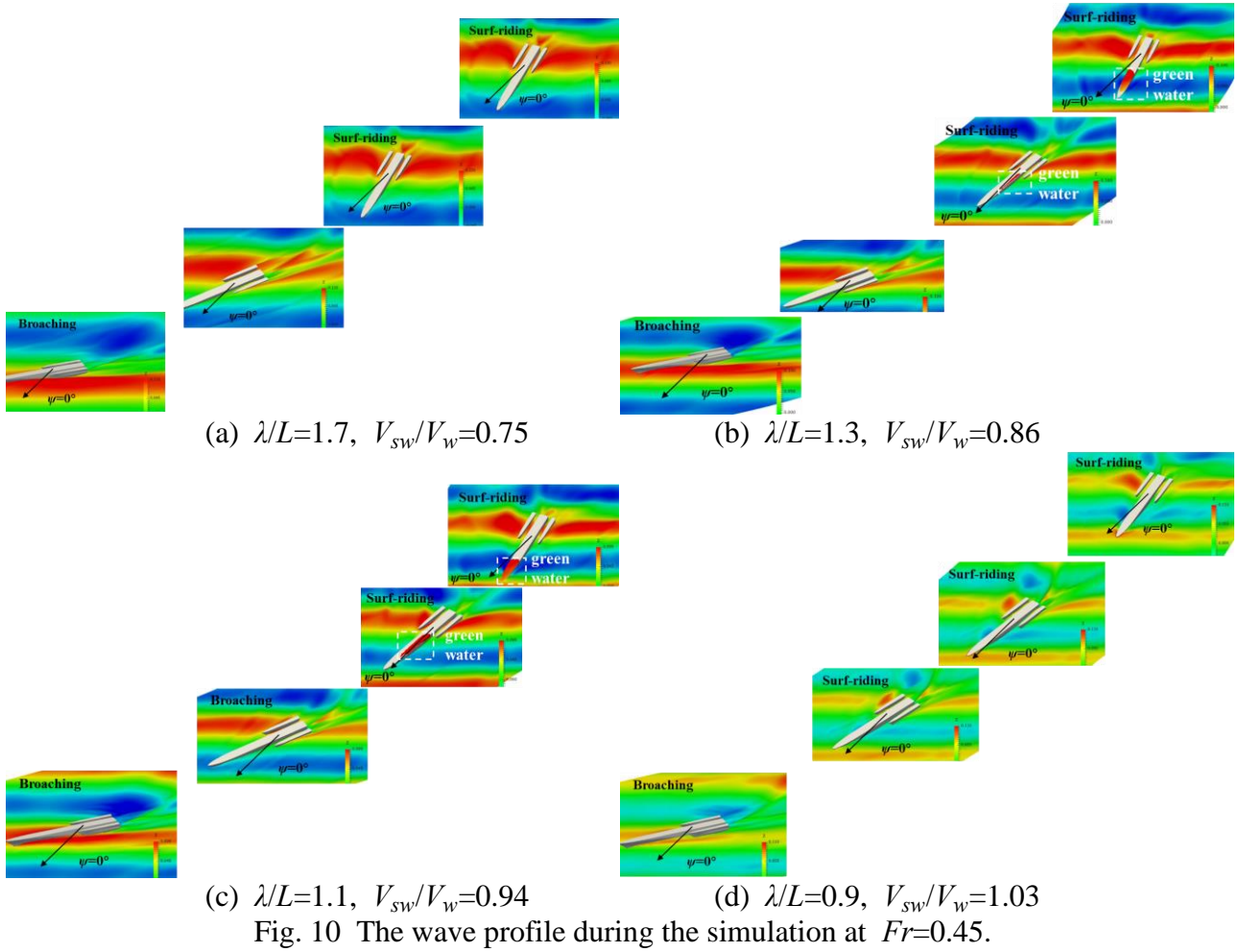


Fig. 10 shows the wave profile of trimaran in different wavelengths captured during the surf-riding and broaching at $Fr=0.45$. In Fig. 10, the marginal broaching occurs in all the wavelengths, but only the $\lambda/L=0.9$ in Fig. 10(d) leads to broaching. It could be seen that no matter how the wavelength varies, a period of surf-riding and a wave peak reaching the stern side could be observed before the trimaran's broach. Sometimes a short time interval could be seen between the surf-riding and broaching, as shown in Fig. 10 (a)(b). During this time interval, the projection speed of the trimaran continues to decrease so that the $V_{sw} < V_w$ and the wave peak could act on the right side hull in a larger area to lead to broaching. By comparing Fig. 10 (a)(b)(c) with (d), it could be found that broaching usually begins with the wave peak acting on the stern of the trimaran. As shown in Fig. 10 (a)(b)(c), the longer wavelength could increase the roll to the portside, which will decrease the effect of the wave on the right side hull, and the larger sinkage of the left side hull is beneficial to reduce the heading deviation at the same time. Besides, broaching ends with the wave peak acting on the bow of the center hull, where the trimaran is of the max positive heave to make the side hulls above water. The larger wavelength is also beneficial in reducing the heading deviation at this time. That is why broaching occurs only in relatively short waves.

383 4 Conclusion

2
3

384 In this paper, the autopilot trimaran in oblique stern waves is simulated by a hybrid method. The
5 6DOF motion and the nonlinear effect are considered, such as the bow-diving, intermittent emergence
385 of side hulls, and green water. The characteristics of the surf-riding and broaching in different working
7
386 conditions are discussed by simulating the trimaran's autopilot with various initial speed and wave
9
387 parameters. The following conclusions can probably be drawn.
11
388

13
389 (1) It is not vulnerable for a trimaran to broaching when moving in small wave steepness. When
15
390 the wave steepness increases to nonlinear waves, a wide range of initial speeds will lead to the
17
391 occurrence of broaching. When the V_{sw}/V_w get closer to 1.0, the trimaran needs to keep the max
18
392 rudder angle for a longer time to change the broaching state. However, the course deviation is still
20
393 more evident at a higher initial speed.
21
22

23
394 (2) The results of the autopilot trimaran in different wavelength and speed shows that, no matter
24
395 how the wavelength varies, no phenomenon of broaching could be observed at a low initial speed
25
396 $Fr=0.35$. When the initial speed is as large as $Fr=0.45$, The marginal broaching appears in a wide
27
397 range of wavelengths, and the broaching could be observed in the wavelength whose wave celerity is
28
398 a bit smaller than the ship projection speed. The wavelength with V_{sw}/V_w close to 1.0 will increase
30
399 the vulnerability of broaching, and the high speed is still an essential factor for broaching.
31
34

35
400 (3) The variation trends of the motion during broaching in different wave parameters and speeds
36
401 are similar. The increase of the heave and decrease of the pitch could be observed. The heel will turn
38
402 from the portside to the starboard for all cases. Though the motion variation is complicated over the
40
403 entire simulation, during the broaching process, the heave is mainly affected by the wave amplitude,
42
404 and the roll and pitch are more sensitive to the wave steepness.

44
405 (4) By current study, it could be found that the steep wave, high speed, and V_{sw}/V_w close to 1.0
46
406 are all necessary conditions for broaching. The broaching of the trimaran usually begins with the
48
407 wave peak acting on the stern, then ends with the wave peak acting on the bow. During the process,
50
408 the two side hulls may have an opposite influence on the heading deviation and broaching. Therefore,
52
409 the position of the side hulls may play an essential role in the trimaran's broaching, and the effect of
54
410 the side hulls on the surf-riding and broaching should be studied in the future.
55

56 5711 Acknowledgment

58
59

6012 This project was supported by the Science and Technology Commission of Shanghai
61
6213 Municipality, China (Grant number 22YF1415900), National Natural Science Foundation of China
63

64
65

1
2 414 (Grant number 51979157).

3
4 415

5
6 416 **Reference**

7

8
9 417 Angelou M., Spyrou K.J., 2021. Broaching-to of sailing yachts. Proceedings of the 1st International
10
11 Conference on the Stability and Safety of Ships and Ocean Vehicles, Glasgow, Scotland, UK.

12
13 419 Begovic E., Bertorello C., Boccadamo G., Rinauro B., 2018. Application of surf-riding and
14
15 broaching criteria for the systematic series D models. *Ocean Engineering*, 170, 246-265.

16
17 421 Gong J.Y., Li Y.B., Jiang F., 2019. Numerical simulation about the manoeuvre of trimaran and
18
19 asymmetric twin hull with hull attitude taken into account by OpenFOAM. *Journal of Marine
20
21 Science and Technology*, 25(3), 769-786.

22
23 424 Gong J.Y., Yan S.Q., Ma Q.W., Li Y.B., 2020. Added resistance and seakeeping performance of
24
25 trimarans in oblique waves. *Ocean Engineering*, 216, 107721.

26
27 426 Gong J.Y., Li Y.B., Cui M., Fu Z., Zhang D.P., 2021. The effect of side-hull position on the
28
29 seakeeping performance of a trimaran at various headings. *Ocean Engineering*, 239, 109897.

30
31 428 Gong J.Y., Li Y.B., Yan S.Q., Ma Q.W., 2022. Numerical simulation of turn and zigzag manoeuvres
32
33 of trimaran in calm water and waves by a hybrid method. *Ocean Engineering*, 253, 111239.

34
35 430 Gu M., Chu J.L., Han Y., Lu J., 2018. Study on vulnerability criteria and model experiment for
36
37 surf-riding/broaching. *Journal of Ship Mechanics*, 22(3), 287-295.

38
39 432 Hu Z., Yan S.Q., Greaves D., Mai T., Raby A., Ma Q.W., 2020. Investigation of interaction
40
41 between extreme waves and a moored FPSO using FNPT and CFD solvers. *Ocean Engineering*,
42
43 206, 107353.

44
45 435 IMO. Finalization of second generation intact stability criteria. Report of the Experts' Group on
46
47 Intact Stability, SDC 6/WP.6, London, UK, 2019.

48
49 437 ITTC, Manoeuvring Committee, 2014. Recommended Procedures and Guidelines. 27th International
50
51 Towing Tank Conference, Copenhagen, Denmark.

52
53 439 Jong P.D., Renilson M.R., Walree F.V., 2013. The broaching of a fast rescue craft in following
54
55 seas. Proceedings of the 12th International Conference on Fast Sea Transportation, Amsterdam,
56
57 Netherlands, December 2013.

58
59 442 Ma Q.W., Yan S.Q., 2009. QALE-FEM for numerical modelling of non-linear interaction between
60
61 3D moored floating bodies and steep waves. *International Journal for Numerical Methods in
62
63 Engineering*, 78(6), 713-756.

64
65 445 Rusche H., 2002. Computational fluid dynamics of dispersed two-phase flows at high phase
66
67 fractions. Imperial College, London, UK.

-
- 447 Pattison D.R., and Zhang J.W., 1994. The Trimaran Ships'. Paper No. 1, RINA Spring Meeting,
2
448 April, 1994.
- 449 Rajendran S., Hassan A., 2019. Surf-riding and Broaching-A numerical investigation on the
5
450 vulnerability of ships. The 5th International Conference on Ocean Engineering, Mauritius.
7
- 451 Renilson M.R. Driscoll, A., 1982. Broaching - An investigation into the loss of directional stability
9
452 in severe following seas. Transactions Royal Institution of Naval Architects, 124, 253-273.
11
- 453 Renilson M.R., Tuite A.J., 1998. Broaching-to - A proposed definition and analysis method.
13
454 Proceedings of the 25th American Towing Tank Conference, Iowa, USA.
14
- 455 Spyrou K.J., Themelis N., Kontolefas I., 2016. Numerical statistical estimates of ship broaching-to.
15
456 Journal of Ship Research 60(04), 219-238.
16
17
- 457 Umeda N., Hamamoto M., 2000. Capsize of ship models in following/quartering waves: physical
20
458 experiments and nonlinear dynamics. Phil. Trans. R. Soc. Lond. A, 358, 1883-1904.
22
- 459 Walree F.V., 2002. Development, validation and application of a time domain seakeeping method
24
460 for high speed craft with a ride control system. Proceedings of the 24th Symposium on Naval
25
461 Hydrodynamics, Fukuoka, Japan.
26
27
- 462 Walree, F.V., Jong, P.D., 2011. Validation of a time domain panel code for high speed craft
29
463 operating in stern quartering seas. Proceedings of the 11th International Conference of Fast Sea
31
464 Transportation, Honolulu, USA.
33
- 465 Weems K., Belenky V., Spyrou K.J., Aram S., Silva K.M., 2020. Towards numerical estimation of
34
466 probability of capsizing caused by broaching-to. 33rd Symposium on Naval Hydrodynamics,
35
467 Osaka, Japan.
36
37
38
- 468 Weller H.G., 2002. Derivation, modelling and solution of the conditionally averaged two-phase
40
469 flow equations. Technical Report TR/HGW/02, Nabla Ltd.
42
- 470 Xing T., Carrica P., Stern F., 2008. Computational towing tank procedures for single run curves of
44
471 resistance and propulsion. Journal of Fluids Engineering, 130(10), 1135-1150.
45
- 472 Yan S.Q., Ma Q.W., 2010. QALE-FEM for modelling 3D overturning waves. Int. J. Numer. Meth.
46
473 Fl., 63, 743-768.
47
48
49
- 474 Yan S.Q., Wang J.H., Wang J.X., Ma Q.W., Xie Z.H., 2019. Numerical simulation of wave
51
475 structure interaction using QaleFOAM. 29th International Offshore and Polar Engineering
53
476 Conference, Honolulu, Hawaii, USA.
54
- 477 Yasukawa H., Hirata N., Kose K., 2005. Influence of outrigger position on the performances of a
55
478 high speed trimaran. Journal of the Japan Society of Naval Architects and Ocean Engineers, 2,
57
479 197-203.
58
59
60
- 480 Yu L.W., Ma N., Wang S.Q., Wang T.H., 2021. Influence of GM on surf-riding and broaching of
62
63
64
65

2
3
4
5
6
7
8
9
10
11
12
13
14
15
16
17
18
19
20
21
22
23
24
25
26
27
28
29
30
31
32
33
34
35
36
37
38
39
40
41
42
43
44
45
46
47
48
49
50
51
52
53
54
55
56
57
58
59
60
61
62
63
64
65